

Supporting Information

for

In situ cross-linked gel polymer electrolyte membranes with
excellent thermal stability for lithium ion batteries

Qin Xiao,† Chun Deng, † Qian Wang, † Qiuqing Zhang,† Yong Yue,† Shijie Ren†*

†College of Polymer Science and Engineering, State Key Laboratory of Polymer Materials
Engineering, Sichuan University, Chengdu, 610065, P. R. China.

* Corresponding Author Email: rensj@scu.edu.cn

CONTENT

Scheme S1. Synthesis strategy of the PS-PEO-PS triblock copolymer.

Figure S1. ¹H NMR spectra of the samples.

Table S1. Molecular weights of PS-PEO-PS block copolymers.

Figure S2. FT-IR spectra of the samples.

Table S2. Porosities of the precursor membranes and cross-linked membranes of CPEs.

Figure S3. DSC curves of the membranes of PVDF and CPEs.

Figure S4. TGA curves of the membranes of PVDF and CPEs.

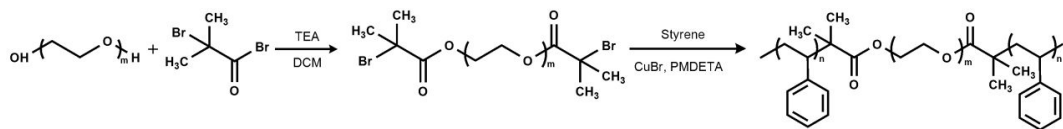
Figure S5. Porosities of pure PVDF membrane under heat treatment at different temperature.

Figure S6. Surface morphology images of the cross-linked membranes of CPEs after the heat treatment at 300 °C.

Figure S7. Cross-section morphology images of the cross-linked membranes of CPEs after the heat treatment at 300 °C.

Figure S8 Charge-Discharge curves of cells at the rate of 0.1 C.

Figure S9 Initial charge-discharge curves of cells at each rates (0.2 C, 0.5 C, 1 C and 2 C).



Scheme S1. Synthesis strategy of the PS-PEO-PS triblock copolymer by ATRP.

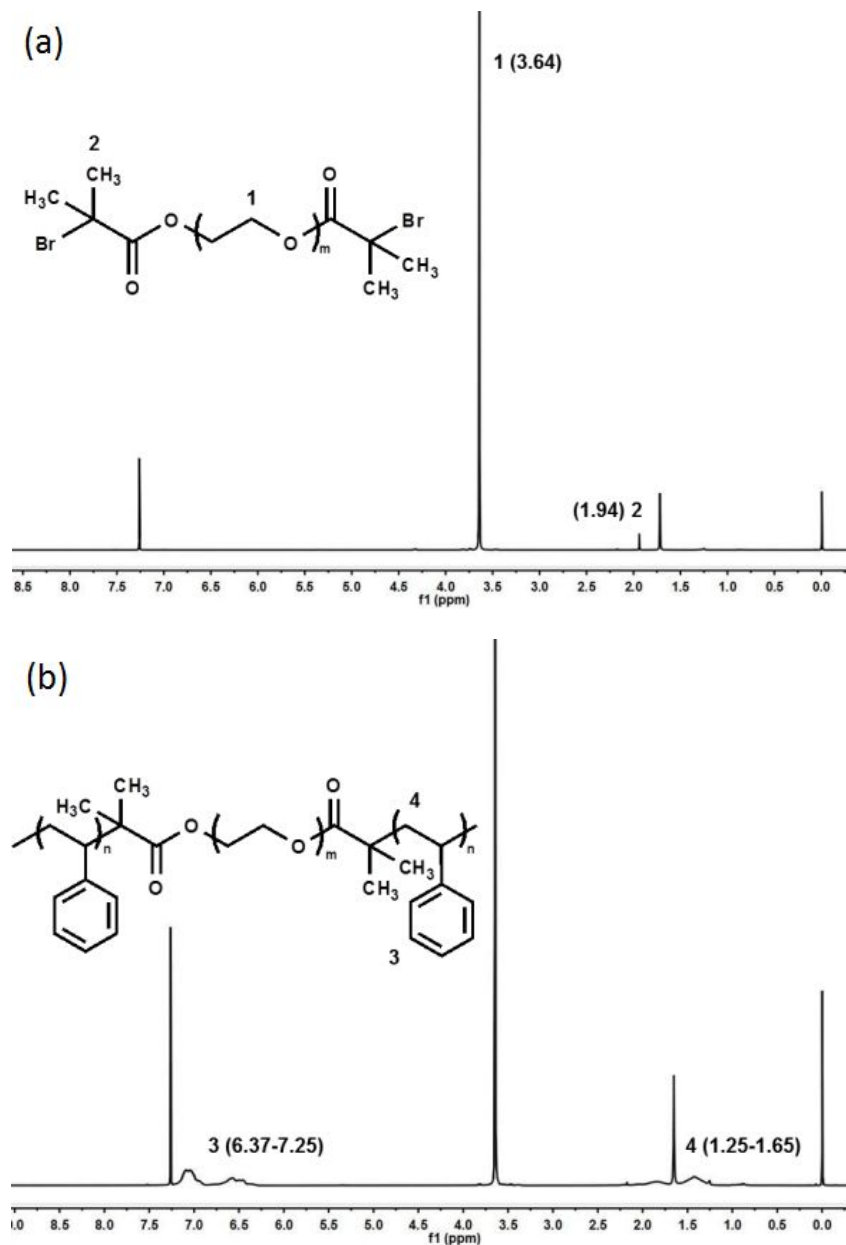


Figure S1. ^1H NMR spectra of (a) Br-PEO-Br macroinitiator, (b) PS-PEO-PS triblock copolymer (taking SES-22 as an example).

Table S1 Molecular weights of PS-PEO-PS block copolymers.

Samples	Copolymer 1	Copolymer 2	Copolymer 3	Copolymer 4	Copolymer 5
$M_{n,total}^*$ (g mol ⁻¹)	11687	13826	22652	36855	61265

$M_{n,total}^*$ was obtained from GPC.

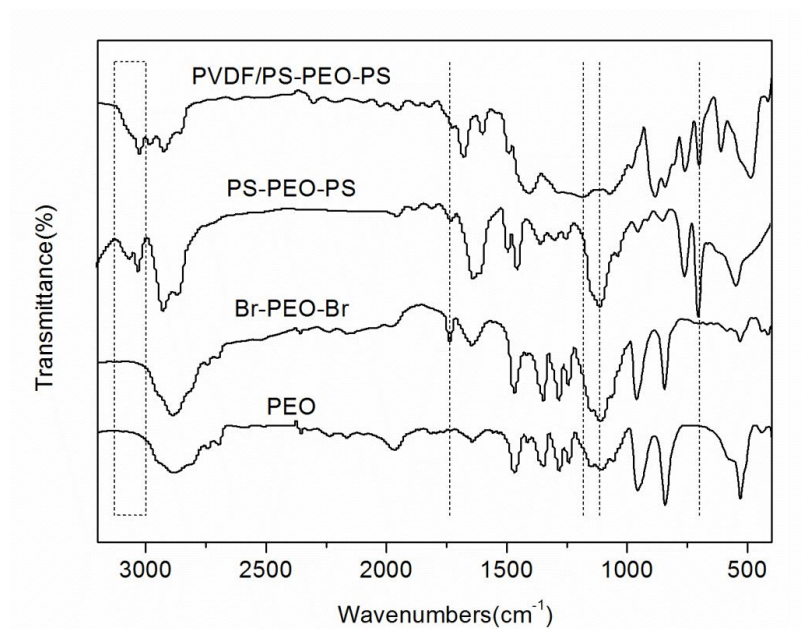


Figure S2. FT-IR spectra of pure PEO, Br-PEO-Br macroinitiator, PS-PEO-PS triblock copolymer and PVDF/PS-PEO-PS precursor polymer (taking Copolymer 2 as an example).

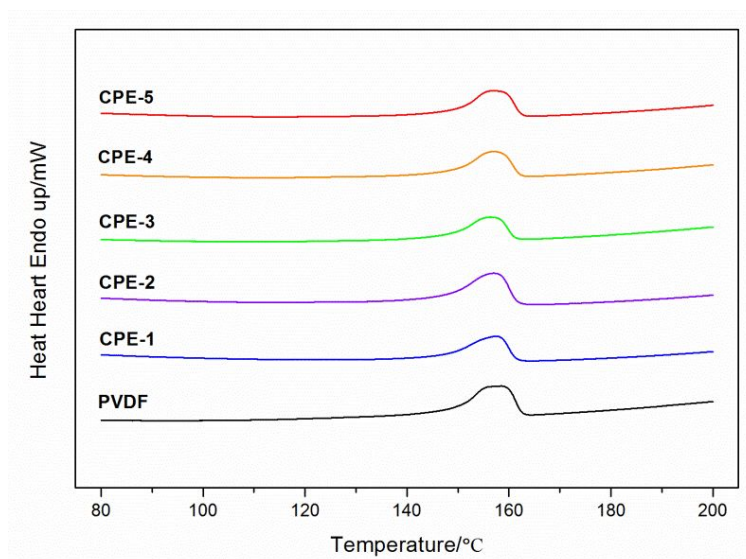


Figure S3. DSC curves of membranes of PVDF, CPE-1, CPE-2, CPE-3, CPE-4 and CPE-5.

Table S2. Porosities of precursor membranes and cross-linked membranes of CPE-1, CPE-2, CPE-3, CPE-4 and CPE-5, respectively.

Samples	Porosity of precursor membranes	Porosity of cross-linked membranes
CPE-1	62.6%	63.7%
CPE-2	62.3%	64.4%
CPE-3	60.8%	63.6%
CPE-4	56.7%	58.3%
CPE-5	44.1%	49.8%

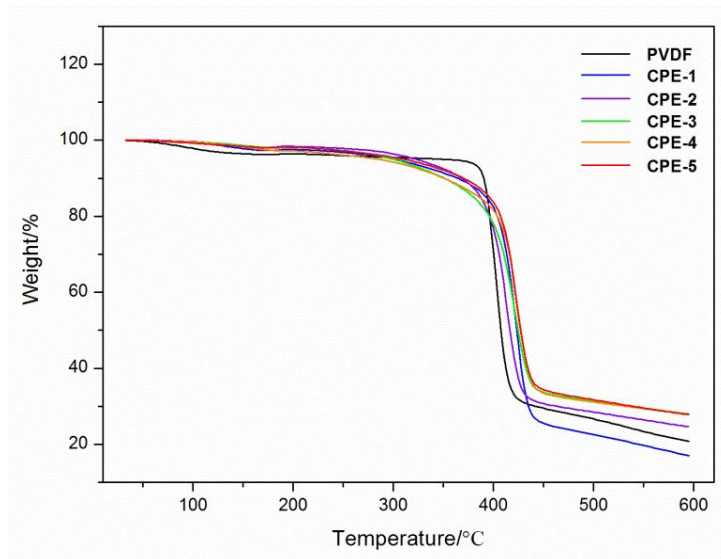


Figure S4. TGA curves of membranes of PVDF, CPE-1, CPE-2, CPE-3, CPE-4 and CPE-5 from room temperature to 600 °C .

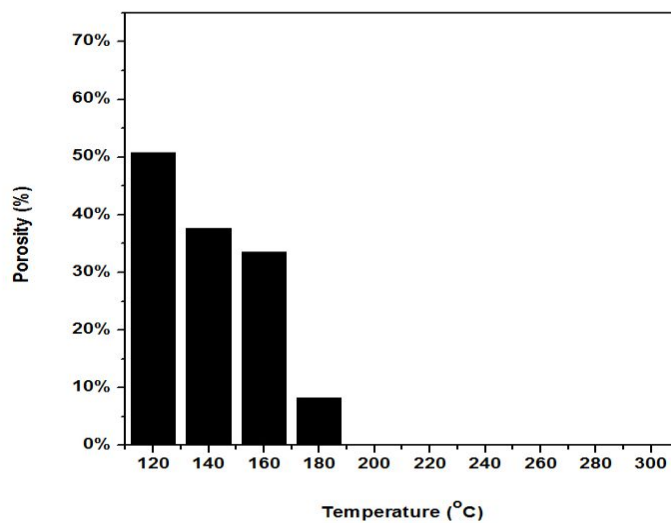


Figure S5. Porosities of pure PVDF membrane under heat treatment at different temperature from 120 °C to 300 °C.

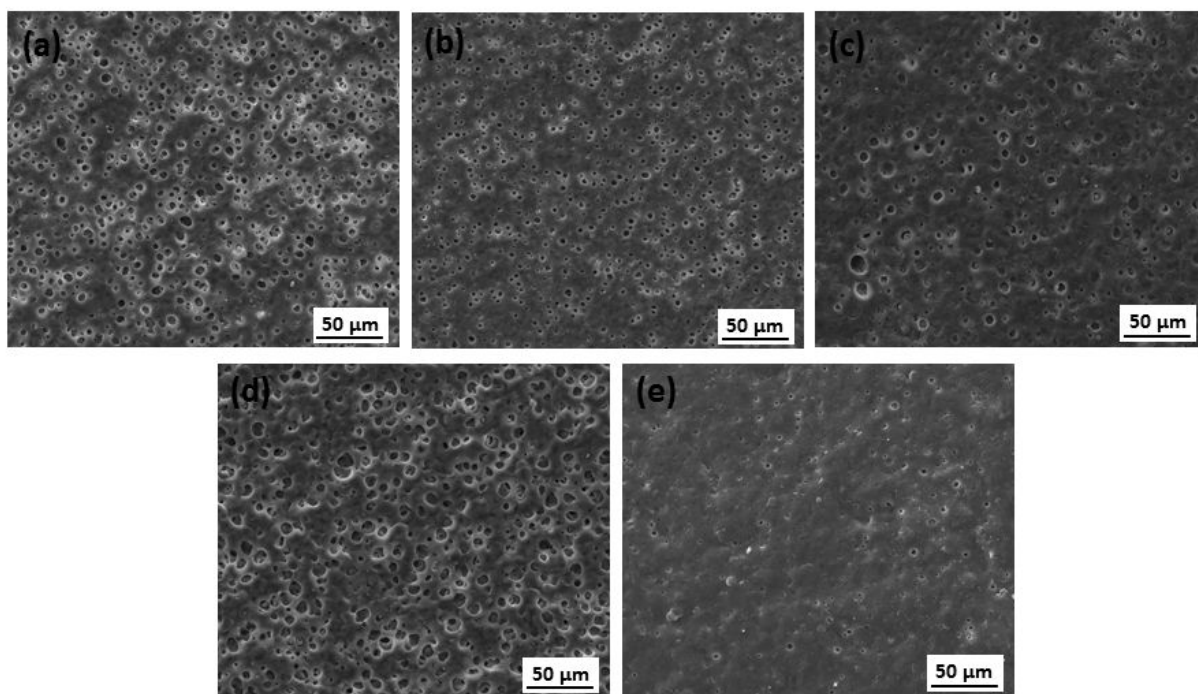


Figure S6. Surface morphology images of the cross-linked membranes of (a) CPE-1, (b) CPE-2, (c) CPE-3, (d) CPE-4 and (e) CPE-5 after the heat treatment at 300 °C.

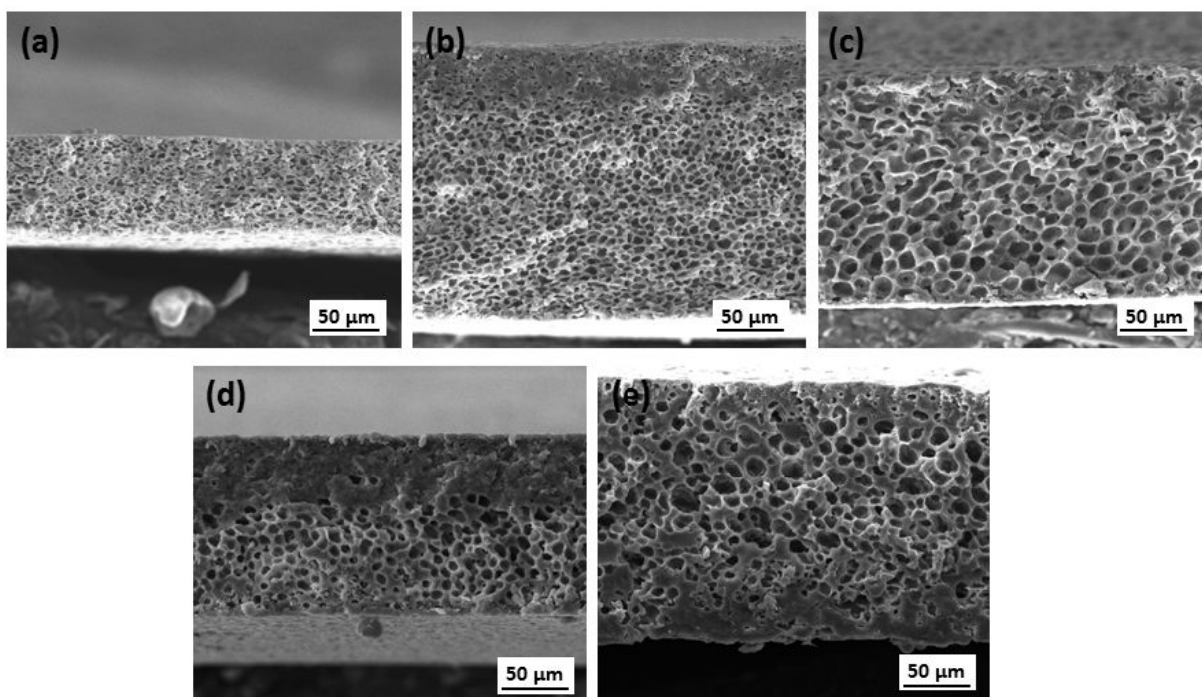


Figure S7. Cross-section images of the cross-linked membranes of (a) CPE-1, (b) CPE-2, (c) CPE-3, (d) CPE-4 and (e) CPE-5 after the heat treatment at 300 °C

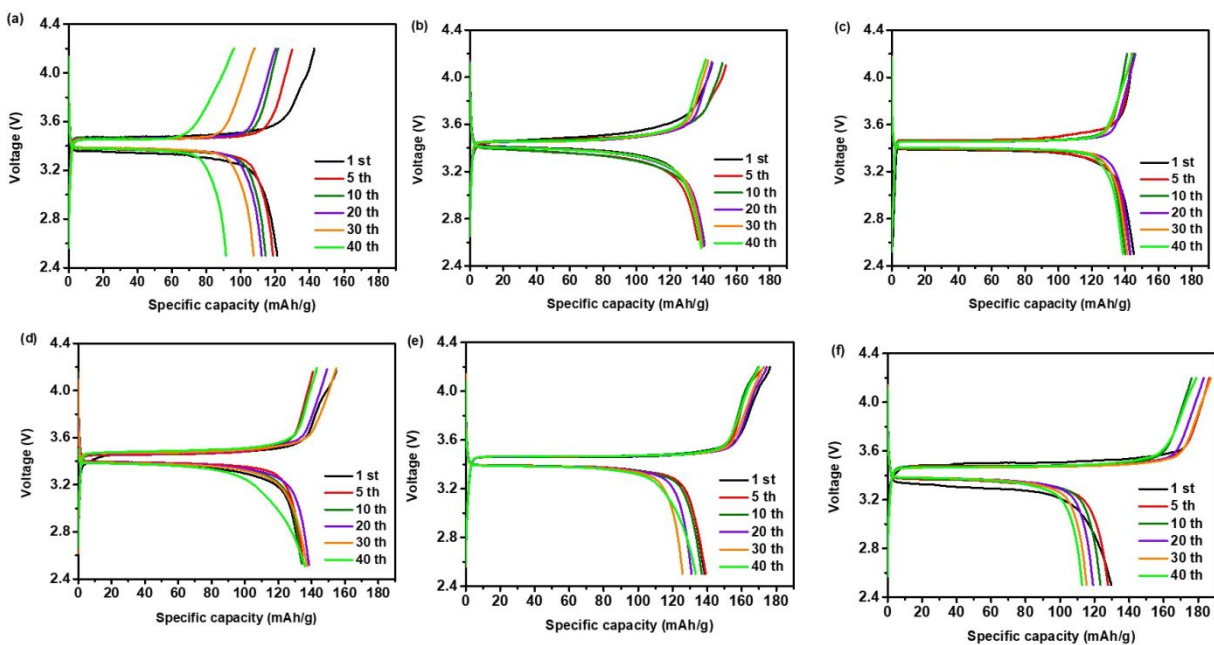


Figure S8. Charge-discharge curves of the cells assembled with (a) PVDF, (b) CPE-1, (c) CPE-2, (d) CPE-3, (e) CPE-4 and (f) CPE-5 at the rate of 0.1 C.

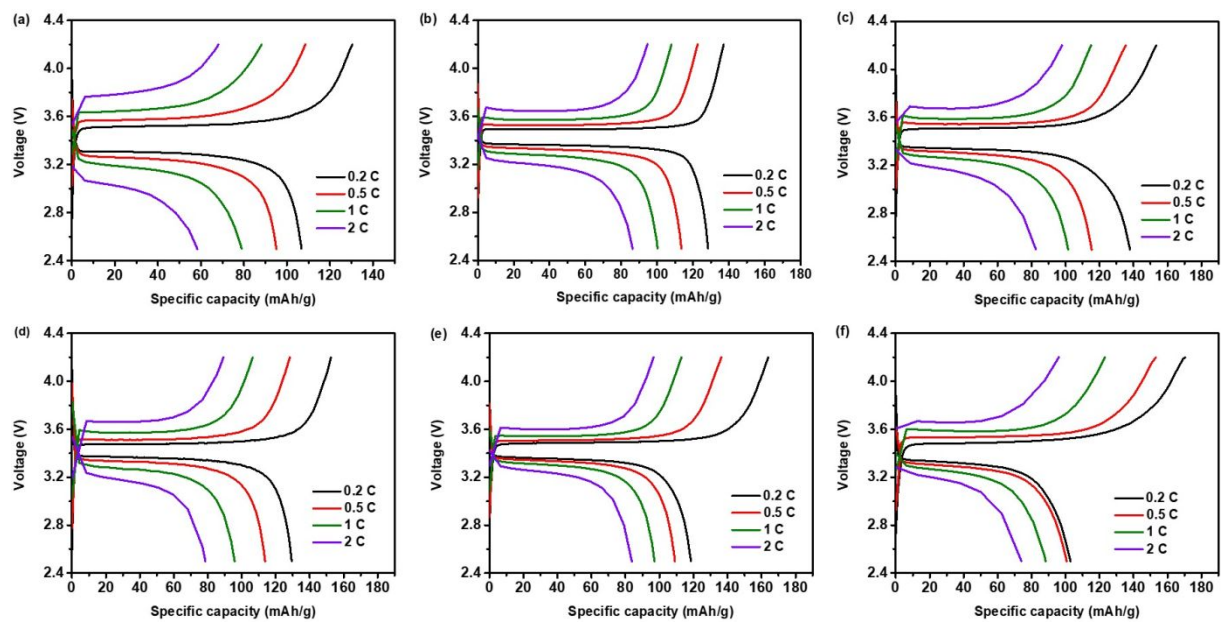


Figure S9. Initial charge-discharge curves of the cells assembled with (a) PVDF, (b) CPE-1, (c) CPE-2, (d) CPE-3, (e) CPE-4 and (f) CPE-5 at varied C rates.